P2-21: Broadband Acoustical Tuning of Nano-Electromechanical Sensors

Florian W. Beil **Achim Wixforth** **Robert H. Blick**

Center for NanoScience and Sektion Physik,
Ludwigs-Maximilians-Universität München
Geschwister-Scholl-Platz 1, 80539 München; Germany
florian.beil@physik.uni-muenchen.de

Abstract

For a variety of applications in integrated communication and sensor devices nano-electromechanical systems (NEMS) present a new generation of high frequency components. Up to now conventional excitation mechanisms for NEMS are based either on high magnetic (magnetomotive method) or electric (electromotive method) fields which limits the use of NEMS. We present experiments utilizing a surface acoustic wave (SAW) transducer on GaAs to excite nanomechanical resonators operating at frequencies up to 300 MHz. We show that via SAW full control over the fundamental properties of the resonator sensor is achieved.

Keywords

Nanomechanical sensors, surface acoustic wave (SAW), driving mechanisms, dissipation control

INTRODUCTION

Implementation of mechanical systems on the micrometer scale (MEMS) nowadays enables sophisticated systems for a variety of sensor and information processing applications [1]. These systems allow on chip solutions whenever low noise and high frequency selectivity is needed. Although, integration and application of MEMS made great progress in recent years, the frequency range interesting for communication systems and single molecule sensors is not achieved by micron scale mechanics. Therefore scaling down to NEMS is desirable, promising an increase of eigenfrequencies far into the lower GHz regime.

Most recent advances give evidence that it is indeed possible to build nanomechanical beam resonators with operating frequencies approaching the GHz barrier and quality factors up to 10^4 and more [2]. The major obstacle limiting integration of NEMS in applications today is due to the lack problem of a suitable excitation mechanism. Currently all driving mechanisms available either depend on high magnetic fields, low temperatures, conductive and hence quite massive layers or electrostatic coupling. This paper presents a technique which brings SAW excitation to use as a mechanical way of fully controlling NEMS overcoming the above drawbacks.

NANO-ELECTROMECHANICAL SENSORS

Nanomechanical systems proofed to reach new standards in detection of ultra small forces and charges. Forces as small as $9.4\cdot10^{-14}$ $N/\sqrt{Hz}$ [3] and sub electronic charges $1.3\cdot10^{-3}$ $e/\sqrt{Hz}$ [3] are detectable. This high resolution finds broad interest in diverse fields of research as well as applications. NEMS with functionalized surfaces enable detection of single molecules and proteins like ion channels [4]. On the other hand measuring single phonon processes [5] and the interaction of single phonons with electrons in freely suspended low dimensional electron systems [6,7] will gain new insight into fundamental physical processes. Furthermore the use of nano beam resonators as low-loss passive frequency filters [8] is of fundamental interest for on chip filters in communication technology, when reaching eigenfrequencies above 1 GHz. Free standing cantilever beams also enable implementation of mechanical single electron transistors operating in the RF regime [9]. Before exploring the implications and difficulties arising when scaling down to the nanometer regime the production and implementation of NEMS are first reviewed.

Nanomechanical Beam Resonators

Preparation of NEMS includes several successive steps of electron beam lithography, anisotropic dry etching and selective isotropic wet etching. The starting material for our purposes is a three layer AlAs/GaAs heterostructure, including a 200 nm thick AlAs sacrificial layer covered by a 300 nm GaAs cap layer. In a first step the beam resonator, input leads and additional structures (e.g. interdigitated transducers (IDTs)) needed for the experiments, are defined using standard E-beam lithography and covered by a 30 nm thick conduction layer (Au). In a subsequent lithographic step the PMMA resist is patterned to form an etch mask for the following reactive ion etching (RIE) step. During this step vertical edges are defined reaching the sacrificial layer at the positions not covered by the PMMA. Carefully timed underetching using 0.1% HF selectively removes the complete AlAs sacrificial under the beam while leaving an AlAs layer under structures with larger lateral dimensions. After the drying procedure the beam remains freely suspended, while other structures are not underetched.

Figure 1 presents an electron beam micrograph of a beam resonator together with an overview of the sample's geometry. The undercut regions are clearly visible, while in the close-up a sidegate is visible, which allows to apply an elec-

trostatic force to the beam resulting in a tuning of the eigenfrequency [10].

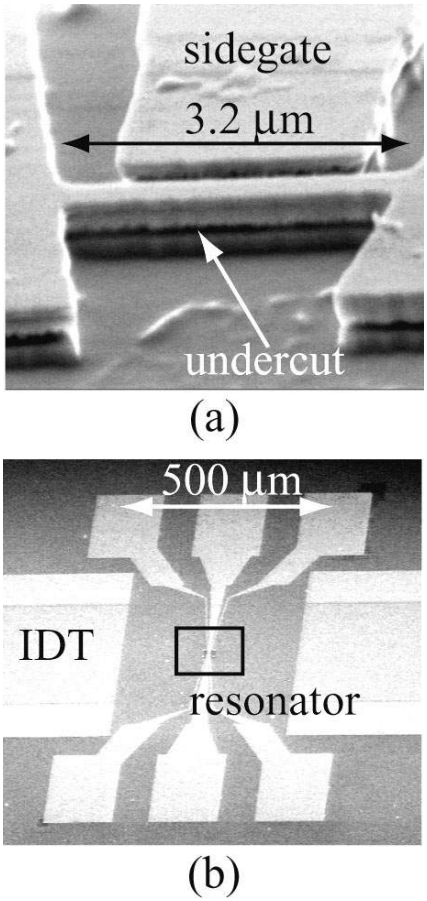

Figure 1. (a) Close-up view of a beam resonator with 3.2 µm length, 300 nm height, and 500 nm width. Close to the freely suspended beam a sidegate is placed. The beam including mechanical supports was matched to a SAW wavelength of 9.2 µm (b) Sample's geometry showing the resonator placed in the path of two interdigitated transducers (ITD) for SAW generation.

Standard theory for clamped beams with the proper boundary conditions yields an inverse quadratic dependence of the eigenfrequency on the length of the beam and a nonlinear dispersion. Resonance frequencies for micromechanical beams can be expressed as [11]

$$f_0 = \frac{1}{2\pi}\sqrt{\frac{k_r}{m_r}} \cong 1.03\frac{h_{eff}}{L^2}\sqrt{\frac{E}{\rho}} \qquad (1)$$

where k_r and m_r are the effective stiffness and mass of the beam at a given position, E and ρ are Young's modulus and the density of the beam's material, L is the length of the beam and h_{eff} is the an effective thickness that models the surface topography of the beam [11, 12]. If the resonator is comprised of two materials Eq. 1 is modified to take into account the elastic constants of both materials [13]. The achievable sensitivity when using beam resonators as sensors scales with the quality factor of the resonator, high resonance frequencies together with low dissipation are desirable.

Driving Mechanisms for Nanomechanics

When scaling mechanical resonators to the nanometer scale one has to be aware of the scalability of the associated driving mechanisms. In principle piezoelectric [14] or electrostatic [3] actuators as well as magnetomotive [3] excitation is feasable, while on the nanometer scale up to now electrostatic coupling via a sidegate and magnetomotive excitation are chosen due the favourable scaling of forces and the difficulties in producing ultra thin piezoelectric films with high quality.

When using magnetomotive excitation the beam is covered by a conduction layer, placed in a strong dc magnetic field and a current is driven along the beam. The induced Lorentz force is used to drive the beam at the resonance frequency. Alternatively the capacitive coupling of the sidegate can be used to exert period forces on the beam. Figure 2 compares the two driving mechanisms.

Beam resonances are detected via standard impedance spectroscopy. The impedance of the resonators is matched to a

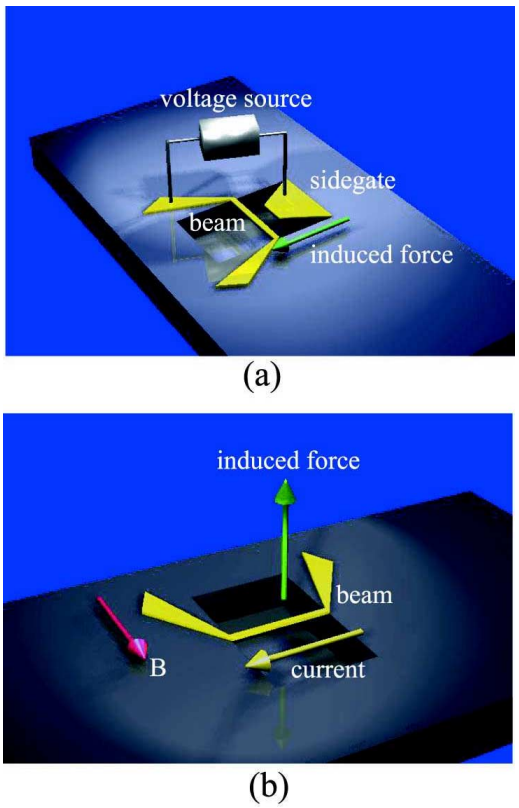

Figure 2. (a) Capacitive driving of beam resonators. The electrostatic coupling of a sidegate is used to exert periodic forces on the resonator. (b) Magnetomotive driving. The induced Lorentz forces of a current driven along the beam excite the beam's motion.

50 Ω strip line circuit. Due to the resonant motion the impedance changes which is detected in the reflected signal using a network analyzer together with a S-parameter test-set. Figure 3 presents a typical measurement of a magnetomotively driven resonator at resonance at ~60 MHz. The dependence of the peak on the magnetic field proofs its mechanical character. In the linear regime the resonances shows Lorentzian shape, while nonlinearities appear when increasing the driving power. The quality factor Q is specified when comparing the resonance frequency ω_0 to the linewidth at half maximum $\Delta\omega$

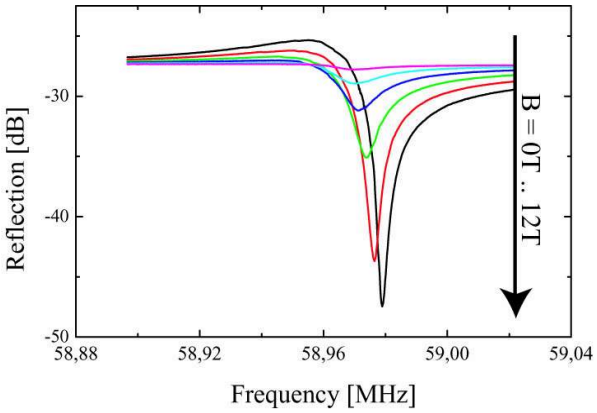

Figure 3. Measured resonance at 59 MHz for increasing magnetic field, applying a power of -52 dBm. The quadratic dependence of peak height on magnetic field proves the mechanical character of the resonance.

$$Q = \frac{\omega_0}{\Delta\omega} \qquad (2)$$

Limitations and Damping mechanisms

So far use of NEMS in commercial applications is difficult due to several reasons concerning the driving mechanisms. For both mentioned actuation schemes the resonator has to be covered by an conducting metal layer which has several negative effects. First of all, when driving the beam magnetomotively ohmic losses occur , decreasing the quality factor and sensitivity of the beam sensor. Second, standard metals like Au or Al have far lower ratios of Young's modulus to material density than the underlying GaAs substrate thus lowering the eigenfrequencies of the composed beam resonator. A third effect is that the internal damping of this resonator is increased due to the inherent damping in thin metal films. It has been shown [15] that damping due to a broad spectrum of tunneling states assigned to dislocations in this metal films can be large and nearly temperature-independent. Applying high magnetic fields for magnetomotive excitation requires low temperatures which makes it unusable for commercial applications.

ACOUSTIC TUNING OF NEMS

An alternative driving mechanism for NEMS without metal layers is found in surface acoustic waves SAW. SAW are acoustic waves propagating at the surface of crystals being able to interact with the surface machined NEMS. Furthermore amplitudes and frequencies of nanomechanical beam resonators lie well in the accessible range for SAW. To develop resonant driving of NEMS by SAW it has to be shown that an interaction is feasible. Subsequent optimizing of this coupling regarding resonant driving will enable a novel acoustic driving mechanism well applicable at room temperature and not depending on conducing layers covering the resonators. Here we will concentrate on the primary interaction of SAW with NEMS while resonant driving will be treated in detail elsewhere [16].

Integration of SAW and NEMS

SAWs are widely used for e.g. filter applications in telecommunication devices. Due to their easy excitation on piezoelectric materials and the adjustability of transfer functions, SAW devices are extensively used in communication devices as well as novel applications like biosensors [17].

SAWs are generated on piezoelectric materials utilizing the inverse piezoelectric effect when applying a voltage to a interdigitated structure (called interdigitated transducer (IDT)). If a voltage is applied to the two electrodes (see Figure 4) the voltage drop between each finger will stress the material beneath. If the input signal meets the resonance frequency

$$f = \frac{v_{SAW}}{\lambda} \qquad (3)$$

,where v_{saw} is the SAW velocity and λ is the lithographically defined double finger spacing of the ITD, a coherent acoustic beam is generated. This situation is depicted in Figure 4, where two IDTs are forming a delayline, whereby one of the IDTs is used to detect the SAW via the accompanying electric fields that cause a potential drop between each finger and enhanced between the electrodes.

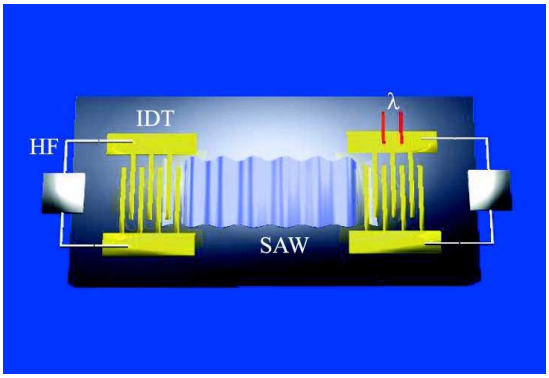

Figure 4. Generation of SAW by IDTs. The frequency of the SAW is defined by via Eq. (3) by the finger spacing of the IDTs.

To investigate the coupling of the SAW to the NEMS we place a beam resonator in the line of fire of two identical IDTs. The beam is driven by standard magnetomotive excitation while the resonance is observed using impedance spectroscopy. Observing the resonance peak of the beam while simultaneously generating the SAW insight into the induced changes upon the resonators characteristic is determined. The experimental setup is depicted in Figure 5. An SEM image of the samples geometry is also shown in Figure 1(b).

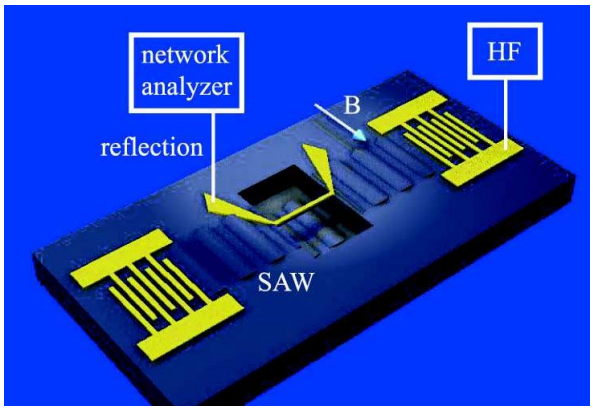

Figure 5. Experimental Setup. The magnetomotively driven beam is placed in the line of fire of two IDTs. The interaction with the SAW is traced via impedance spectroscopy using a network analyzer.

Coupling NEMS via SAW

In the experiments we investigated the resonance shown in Figure 3 and trace its changes when applying the SAW. Figure 6 shows the main experimental observations. In Figure 6(a) the spectrum of the generated SAW is plotted, showing a $\sin(f)/f$ dependence around the frequency of maximal SAW generation. In Figure 6(b) lines of the beam resonance are plotted in dependence of the frequency applied to the IDT. We observe a shift and a strong attenuation of the beam's resonance appearing when the driving signal at the IDT meets condition Eq. (3) for resonant SAW excitation. This effect is demonstrated more pronounced when plotting the resonators Q in dependence on the frequency of the IDTs input signal. The insets of Figure 7 shows how the amplitude and the center frequency of the resonance is tuned by the SAW.

To exclude that these effects are solely induced by a local heating of the material by the SAW we estimated the temperature required to result in the observed shift of the resonators eigenfrequency by softening of the elastic constants [18, 19]. This temperature is about 40 K which is far beyond previously observed SAW crystal heating effects [20]. Excluding thermal heating the SAW tuning of the beam's resonance is assigned to mechanical coupling of the SAW to the resonator's mode. This proofs that it is possible to couple mechanically to the beam and , in optimizing this coupling, to drive the beam via acoustic excitation. As frequency and phase matching of SAW to the beam is difficult, pulsed SAW excitation is more favourable for driving purposes. This is demonstrated elsewhere [16].

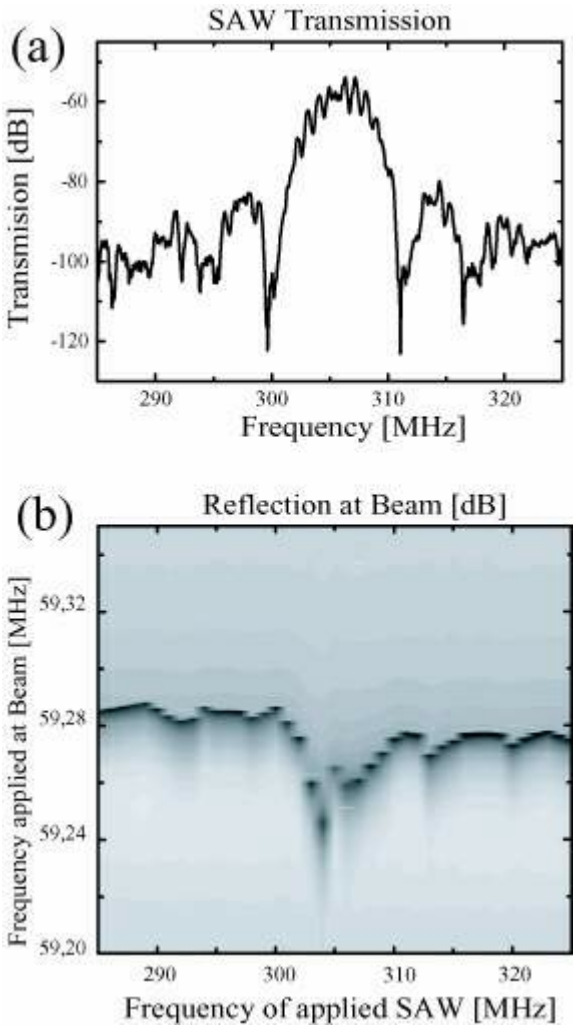

Figure 6. (a) SAW transmission over the IDT delay-line. The spectrum shows a typical sin(f)/f dependence with a maximal SAW generation at 305 MHz (b) SAW induced changes in the resonance of the beam. The observed shifts corresponds to the SAW generation seen in (a).

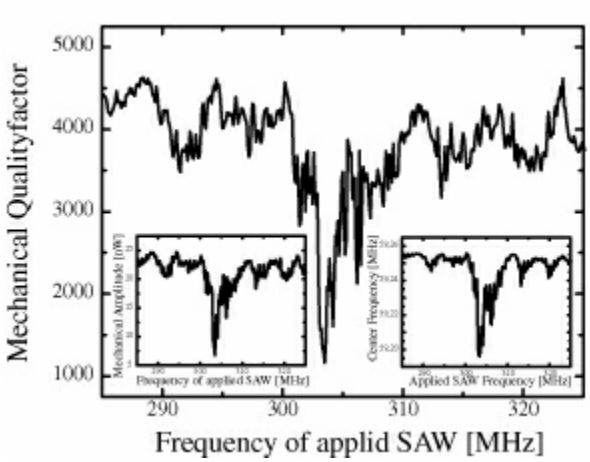

Figure 7. Tuning of the quality factor by the SAW. The insets show the amplitude and the center frequency of the resonance respectively.

The dramatic decrease of the resonator's quality factor is a proof that it is also possible to dynamically tune the dissipation in NEMS by SAW. We believe that this increased dissipation is caused by an increased thermoelastic damping in the beam due to the SAW induced time-dependent additional stress in the beam [21]. Again pulsed SAW excitation will allow to study the dynamics of this damping mechanisms in NEMS.

CONCLUSIONS

We have shown that coupling of SAWs to a nanomechanical beam resonators offers the possibility for a novel room temperature driving mechanism, free of ohmic losses and damping induced by metal layers. The results show that it is further possible to dynamically tune the beams dissipation mechanisms enabling time resolved experiments that scan the dynamics of internal dissipation mechanism, thus allowing further improvement of the resonators quality factor. Having sensoric applications in mind, the increased resolution due to ultra high quality factors will allow applications of SAW driven NEMS at room temperature reaching sensitivities that allow e.g. detection of single molecule events.

ACKNOWLEDGMENTS

We thank J.P. Kotthaus and M.L. Roukes for continuous discussion and A. Kriele, K. Wehrhahn, and S. Manus for technical support. We acknowledge financial support by the Deutsche Forschungsgemeinschaft through grant DFG/Bl-487/3.

REFERENCES

[1] A.-C. Wong, H. Ding, and C. T.-C. Nguyen, 'Micromechanical mixers and filters'', *Technical Digest*, IEEE International Electron Devices Meeting, San Francisco, California, Dec. 6-9, 471 (1998).

[2] F. W. Beil, A. Wixforth, R. H. Blick, 'Investigation of nano-electromechanical systems using surface acoustic waves', Physica E, article in press

[3] F. W. Beil, L. Pescini, E. M. Höhberger, A. Kraus, A.Erbe, and R. H. Blick, 'Comparing schemes of displacement detection and subharmonic generation in nanomachined mechanical resonators', submitted to IEEE JMEMS

[4] N. Fertig, A. Tilke, R.H. Blick, J.P. Kotthaus, J.C. Behrends, G. ten Bruggencate, 'Stable integration of isolated cell membrane patches in a nanomachined aperture: a step towards a novel device for membrane physiology', Appl. Phys. Lett. 1218, 77 (2000).

[5] M. L. Roukes, 'Yoctocalorimetry: phonon counting in nanostructures', Physica B, 263-264, 1-15 (1999)

[6] R.H. Blick, F.G. Monzon, W. Wegscheider, M. Bichler, F. Stern, M.L. Roukes, "Magnetotransport on freely Suspended Two-Dimensional Electron Gases", Physical Review B, 17103, 62 (2000).

[7] J. Kirschbaum, E. M. Höhberger, R. H. Blick, W. Wegscheider and M. Bichler, 'Integrating suspended Quantum Dot Circuits for Applications in Nanomechanics', submitted to Appl. Phsy. Lett. (2002).

[8] C. T.-C. Nguyen, 'Vibrating RF MEMS for low power wireless communications (invited)', Proceedings; 2000 Int. MEMS Workshop (iMEMES'01) Singapore, July 4-6, 2001, pp. 21-34

[9] A. Erbe, C. Weiss, W. Zwerger, and R. H. Blick"Nanomechanical Resonator Shuttling Single Electrons at Radio Frequencies", Phys. Rev. Lett. 87, 096106 (2001).

[10] Andreas Kraus, Artur Erbe, Robert H. Blick, Gilberto Corso, and Klaus Richter, "Parametric frequency tuning of phase-locked nanoelectromechanical resonators", Appl. Phys. Lett. 79, 3521 (2001).

[11] F. D. Bannon III, J. R. Clark, and C. T.-C. Nguyen, 'High frequency micromechanical filters', IEEE J. Solid-State Circuits, vol. 35, no. 4, pp. 512-526 (2000)

[12] Q. Meng, M. Mehregany, and R. L. Mullen, 'Theoretical modelling of microfabricated beams with elstically restrained supports', J. Micorelectromech. Syst., vol. 2, no. 3, pp. 128-137 (1993)

[13] Y. T. Yang, K. L. Eknici, X. M. H. Haung, L. M. Schiavone, and M. L. Roukes, C. A. Zorman and M. Mehregany, 'Monocrystalline silicon carbide nanoelectromechancial systems', Appl. Phys. Let.78,2 162 (2001)

[14] D. L. DeVoe, 'Piezoelectric thin film micromachined beam resonators', Sensors and Actuators A 88 263-272 (2000)

[15] X. Liu, E. Thompson, B. E. White, Jr., and R. O. Pohl, 'Low-temperature internal friction in metal films and in plastically deformed bulk aluminium', Phys. Rev. B 59,18 (1999)

[16] F. W. Beil, A. Wixforth, and R. H. Blick, to be published.

[17] A. Rathgeber, C. Strobl, H.-J. Kutschera, and A. Wixforth, 'Planar microfluidics - liquid handling without walls', to be published.

[18] J. R. Neighbours and G. A. Alers, 'Elastic Constants of Silver and Gold', Phy. Rev. 111,3 707-712 (1958)

[19] R. I. Cottam and G. A. Saunders, 'The elastic constants of GaAs from 2 K to 320 K', Journal of Physics C **6**, pp. 2105-2118 (1973)

[20] A. Wixforth, J. Scriba, M. Wassermeier, and J. P. Kotthaus, 'Surface acoustic waves on GaAs/$Al_xGa_{1-x}As$ heterostructures', Phys. Rev. B 40/11, pp. 7874-7887 (1989)

[21] R. Lifshitz and M. L. Roukes, 'Thermoelastic damping in micro- and nanomechanical systems', Phys. Rev. B 61/8, pp. 5600-6090 (2000).